In situ localization of micropollutants and associated stress response in Populus nigra leaves

Claire Villette, Loïc Maurer, Julien Delecolle, Julie Zumsteg, Mathieu Erhardt, Dimitri Heintz

In situ localization of micropollutants and associated stress response in *Populus nigra* leaves.

Authors
C. Villette[a†*], L. Maurer[a,b†], J. Delecolle[a], J. Zumsteg[a], M. Erhardt[c], D. Heintz[a]

Affiliations
[a]Plant Imaging and Mass Spectrometry (PIMS), Institut de biologie moléculaire des plantes, CNRS, Université de Strasbourg, 12 rue du Général Zimmer, 67084 Strasbourg, France.

[b]Département mécanique, ICube Laboratoire des sciences de l'ingénieur, de l'informatique et de l'imagerie, UNISTRA/CNRS/ENGEES/INSA, 2 rue Boussingault, 67000 Strasbourg, France.

[c]Microscopie et imagerie cellulaire, Institut de biologie moléculaire des plantes, CNRS, Université de Strasbourg, 12 rue du Général Zimmer, 67084 Strasbourg, France.

[†]These authors contributed equally to this work
*corresponding author
claire.villette@ibmp-cnrs.unistra.fr

Abstract

Micropollutants and emerging organic contaminants (EOCs) have been widely studied in terms of persistance, removal, human risk assessment, toxicology, etc. Mass spectrometry imaging (MSI) offers the possibility of following the fate of a single pesticide in a plant leaf or a drug in the whole body of an animal, organ by organ. However, the admissibility of chronic low doses of complex mixtures for the ecosystem has not been assessed. How do micropollutants diffuse in the environment? How do living organisms cope with chronic exposure to a low dose of diverse miropollutants? Is there a cocktail effect or a chance for hormesis? Combining mass spectrometry imaging (MSI) and targeted and nontargeted liquid chromatography coupled to mass spectrometry (LC-MS), we attempt to answer these questions. We investigate the diversity of micropollutants at the exit of a water treatment facility, their diffusion in sludge and black poplar (*Populus nigra*), and their impact on a living organism. We reveal a specific tissue localization of micropollutants in peripheral leaf tissues, and an associated stress response from the plant, with stress hormones and tissue degradation markers induced in the plant growing near the water efflux.

Keywords

Populus nigra; waste water; sludge; constructed wetland; micropollutants; mass spectrometry imaging (MSI).

1. Introduction

Micropollutants and emerging contaminants are an increasing focus of national and international laws (for example, Clean Water Act, Water Framework Directive), as their impact on human health is important. These compounds are released by human activities (agriculture, cosmetics, drugs, industry, etc.) and reach the environment in part through urban wastewater, making it essential to improve its depollution, and to understand the impact on the receiving ecosystem after treatment. Some pollutants have been deeply studied to investigate their mode of action, to facilitate their better use and to reduce the amounts spread in fields. However, micropollutants have been shown to be present in the environment not only as their original form but also as metabolites, which have been less studied in terms of effects on living organisms and toxicity. For example, some studies have shown the vast diversity of metabolites that a plant can produce from a single molecule such as ibuprofen (Marsik et al., 2017). As plants are the first step in the food web, there is a risk that these micropollutants and their metabolites will diffuse and reach humans, either through the grass grazed on by herbivores raised to feed humans or by direct consumption of edible plants amended with manure. This phenomenon was well documented in the case of crop species (Adeel et al., 2017; Prosser and Sibley, 2015; Wang et al., 2018). In contrast, few studies have focused on the effect of micropollutants accumulation in spontaneous species and more generally on living organisms established near the exit of water treatment facilities. We investigated the presence of micropollutants in major compartments of the environment: water, sludge and plant, providing a large overview of the health of the environment at the release point of the treated water. We chose black poplar (*Populus nigra*) as a model species to investigate the potential accumulation of micropollutants in plant tissues and the effects that could be linked. Black poplar is a spontaneous species growing in the European climate, which grows on river banks. *P. nigra* is known to display rapid growth and a high evapotranspiration rate (Guidi et al., 2008), and thus, we considered it to nicely reflect the potential micropollutants accumulation as high amounts of water, possibly polluted, would be used for growth by this plant. Moreover, this species is well known for its capacities in phytoremediation (K. Y. Lee et al., 2012) and heavy metals removal (Jakovljević et al., 2014). However, to our knowledge, no inventory of micropollutants occurring in poplar leaves in field conditions has been published. Additionally, the tissue localization of such micropollutant accumulation in plant leaves has never been investigated in a nontargeted way, allowing the identification of plant metabolites in response to this accumulation without any *a priori* knowledge. Thus, we used mass spectrometry imaging (MSI), also called matrix assisted laser desorption ionisation (MALDI) imaging. This technique is widely used to study plant biology (Bhandari et al., 2015; Bjarnholt et al., 2014; Kulkarni et al., 2018; Y. J. Lee et al., 2012), but

it has also been discussed as an efficient tool for the toxicological evaluation of environmental pollutants (Anderson et al., 2010; Fernandes et al., 2018; Lagarrigue et al., 2016; Rivas et al., 2017). It allows the *in situ* localization of metabolites and, therefore, is a valuable tool for understanding biological processes in whole organs or organisms. In this study, we used high resolution MSI to investigate the metabolic profile of a black poplar growing on the bank of a ditch wetland, situated at the exit of a two-stage vertical flow constructed wetland. This poplar is confronted by chronic exposure to micropollutants. Moreover, we were able to implement a control in a field experiment, which is often lacking due to experimental constraints. This control poplar only benefits from water supplied by the rain, as a drainage is set up in the wetland. Thus, we demonstrate the role of plants in micropollutants sequestration, as well as their biological response to pollutants accumulation in an active manner, using *P. nigra* as a model species.

2. Materials and Methods

2.1. Experimental design

The study was conducted in the wetland situated in Falkwiller, Alsace, France. Two poplar trees were planted two years before the beginning of the samplings to obtain a "polluted" poplar growing near the water exit, and a control poplar receiving only rain water. Eight biological replicates of each condition (control *vs* polluted) were prepared for liquid chromatography and pigments analysis, and 5 biological replicates were prepared for MSI analysis, using different leaves from a single tree for each condition (control *vs* polluted). The samples were collected in September 2017, after a full season of plant growth, and before senescence. The objectives of this research were to investigate the types of molecules found in three compartments of the environment: water, soil and plants, with a focus on the tissue localization in plant leaves and the plant response. To achieve this goal, we used LC coupled to high resolution mass spectrometry (HRMS) to draw a large-scale metabolic profile of the different compartments studied. Public databases were used to annotate the metabolic features found, and manual curation revealed 11 major classes of compounds in the matrices. The tissue localization of micropollutants and plant metabolites in poplar leaves was investigated by MSI, using the advantage of a control plant to search the discriminative metabolites that are mostly found in polluted poplar leaves, either micropollutants or plant metabolites. The hormonal profile of the trees was also investigated to search for a plant response to chronic exposure to low doses of micropollutants.

2.2. Biological material

All biological materials were obtained from the waste water treatment plant situated in Falkwiller (Alsace, France) which is composed of a two-stage vertical flow constructed wetland (VFCW) planted with reeds (*Phragmites australis*) and a tertiary treatment wetland (ditch) colonized by spontaneous

plant species. It is the oldest VFCW associated with a tertiary wetland in Alsace (2009). Two black poplars (*Populus nigra*) were planted for the experiment: one on the bank at the entrance of the ditch (denoted polluted), and one on the top of a bund situated 16 meters away from the ditch (denoted control). Water, sludge and polluted poplar were obtained from the same square meter at the ditch entrance. Surface water (0-15 cm) and superficial sludge samples (10 cm depth) were collected in glass bottles (2 L), sampled at 4°C and stored at 4°C before sample preparation. Plant material was sampled at 4°C and stored at -20°C before sample preparation. The area of the leaves was measured using the area measurement tool of ImageJ software (Schneider et al., 2012) on five leaf replicates for each condition.

2.3. Chemicals

Sildenafil-d3, sulfamethoxazole-d4, N-desmethyl sildenafil-d8, bezafibrate–d4, diclofenac-d4, and gemfibrozil-d6 standards were purchased from Toronto Research Chemical (Ontario, Canada), and acetaminophen-d4 standard was purchased from Sigma Aldrich to determine the limits of detection (LOD) and quantification (LOQ) in the different matrices. Solvents (acetonitrile, methanol and isopropanol) were purchased from Fisher Chemicals (New Hampshire, USA). Acetone, formic acid and acetic acid were obtained from Sigma Aldrich (Missouri, USA), ammonium formate from Fluka Analytical (Missouri, USA) and NaOH from Agilent Technologies (California, USA). Deionised water was obtained from a Direct-Q UV (Millipore, Massachusetts, USA) station. The internal standard for plant samples was deuterated abscisic acid ($^2H_6$ ABA) from OlChemIm (Olomouc, Czec republic). Tentative identifications were confirmed using piperidine (Sigma), ethylene thiourea (TCI chemicals, Paris, France), 3-ethoxypropylamine (Sigma), adenine (Sigma), D-salicin (Sigma), lysoPC(16:0) (Avanti Polar Lipids, Alabama, USA) and pheophorbide a (Santa Cruz Biotechnology, Texas, USA) as standards.

2.4. Water and sludge extraction process

Water was filtered with a paper filter as a pretreatment to eliminate coarse particles. Then, 50 mL of the sample was used for micropollutant analysis as described in (Cotton et al., 2016). Internal standards as described in Boleda et al., (2013) were added to the samples to calculate the limits of detection (LOD) and quantification (LOQ). Water samples were freeze-dried using a speedvac concentrator (Savant SPD121P, Thermo Fisher) and resuspended in 1mL of methanol:water (90:10). Solvents used for extraction were chosen according to Nuel et al., (2018). Sludge samples were filtered with a paper filter to eliminate the aqueous phase. A double extraction was applied to 10 g of the sludge samples. The first overnight extraction was carried out under shaking at 4°C using 40 mL of acetonitrile:water (90:10) with 1% acetic acid. Samples were centrifuged for 15 minutes at 5500 rpm.

The supernatant was recovered and freeze-dried. The second extraction was performed under shaking at 4°C for 15 minutes using 20 mL of isopropanol:acetonitrile (90:10). The samples were centrifuged again, and the supernatant was recovered and pooled with the first extraction to be freeze-dried. Finally, the samples were solubilized in 1 mL of acetonitrile:isopropanol:water (50:45:5). All samples were extracted in triplicate. The samples were concentrated (10-fold) and diluted (2; 10; 20; 100; 200 and 1000-fold) to obtain a global vision of the micropollutants present.

2.5. Method assessment

The repeatability of the extraction process was determined using the same labeled standards and searching for the area of the peaks on three technical replicates for each matrix. Limits of detection (LOD) and quantification (LOQ) were defined using labeled internal standards spiked in water and sludge matrices from 1 $ng.mL^{-1}$ to 10 $\mu g.mL^{-1}$. The signal/noise ratio (S/N) value was used as a threshold, and the limit of detection was reached at S/N=3 and limit of quantification at S/N=5.

2.6. Poplar leaf extraction process

Frozen poplar leaves were weighed to 300 mg fresh weight and ground in liquid nitrogen. Then, 1.5 mL cold MeOH (4°C) containing $^{2}H_{6}$ abscisic acid as an internal standard (1 $\mu g.mL^{-1}$ final in the samples) was added to the leaf powder, vortexed, incubated overnight (16 h) at -20°C and centrifuged for 15 minutes at 13 000 rpm, 4°C. The supernatant was recovered in a glass vial and evaporated using a speedvac concentrator at room temperature (Savant SPD121P, Thermo Fisher). The extraction process was then repeated once with pure MeOH (4°C). The supernatant recovered at each step was pooled in the same glass vial for each sample. Finally, the dried material was recovered in 300 µL of MeOH. Eight biological replicates were assessed for each condition (control and polluted), using different leaves from a single tree for each condition.

2.7. Pigment extraction and quantification

Poplar leaves (20 mg fresh weight) were ground in fresh 80% acetone with metal beads for 2 minutes at 30 Hz (Tissue Lyser, Qiagen, Hilden, Germany). The samples (eight replicates for each condition) were then incubated in the dark at 4°C for 24 h. The optical density of the samples was measured at 470 nm, 646 nm, 663 nm with FLUOstar Omega spectrometer (BMG Labtech, Ortenberg, Germany) in a 96-well microplate (96-well ELISA microplates, PS, U-bottom, MICROLON®, Greiner Bio-one, Kremsmünster, Germany) containing 200 µL of the diluted samples (10 times) and 80% acetone as a blank. The concentration of chlorophyll a (a), chlorophyll b (b) and carotenoids (xantophylls and carotenes, c+x) was determined using the equations described by Lichtenthaler and Buschmann, 2001:

157 c_a (µg/mL) = 12.25 $A_{663.2}$ – 2.79 $A_{646.8}$

158 c_b (µg/mL) = 21.50 $A_{646.8}$ – 5.10 $A_{663.2}$

159 $c_{(x+c)}$ (µg/mL) = (1000 A_{470} – 1.82 c_a – 85.02 c_b)/198

160

161 *2.8. Hormone analysis*

162 Plant hormones were analyzed in leaf extracts as described in Villette et al., (2018). Briefly, 15 mg of
163 dried leaf material was ground with metal beads and extracted three times with 1.5 mL of MeOH. The
164 supernatant was recovered and dried, and the three extractions were pooled in the same glass vial. The
165 pellets were recovered in 100 µL of methanol to be analyzed by liquid chromatography on a C_{18} HSS
166 T3 column coupled to mass spectrometry in positive and negative ion modes by multiple reaction
167 monitoring (MRM). $^2H_6$ ABA was used as an internal standard, which was spiked during the first
168 extraction.

169

170 *2.9. Transmission electron microscopy (TEM) sample preparation*

171 Fresh leaves were collected, fixed with 3% glutaraldehyde and stored overnight at 4°C before sample
172 preparation. The leaves were then treated with 0.1% osmium tetroxide and stained with 2% uranyl
173 acetate. The samples were dehydrated *via* ethanol series and infiltrated with EPON812 medium grade
174 resin (Polysciences, Germany). Polymerization was performed over 48 h at 60°C. Ultrathin sections
175 were cut using an ultracut E microtome (Reichert, Germany) and collected on grids coated with
176 formvar (EMS, Washington). Observations were carried out with a Hitachi H7500 electron
177 microscope at 80kV. Images were captured with a CCD Advantage HR Hamamatsu camera and AMT
178 software (AMT, Danvers).

179

180 *2.10. LC-Q-TOF-HRMS analysis*

181 Water, sludge and plant extracts were analyzed using liquid chromatography (LC) coupled to high
182 resolution mass spectrometry (HRMS) on a DioneX Utlimate 3000 (Thermo) coupled to a Q-TOF
183 Impact II (Bruker) using the TargetScreener method developed by Burker (Bremen, Germany). This
184 method was already used by Bergé et al., (2018), it allows the targeted identification of drugs and
185 pesticides, but the data can also be investigated for untargeted analysis. Solvent A was composed of
186 H_2O:MeOH (90:10), 0.01% formic acid and 314 mg.L^{-1} ammonium formate. Solvent B was composed
187 of MeOH, 0.01% formic acid, and 314 mg.L^{-1} ammonium formate. Samples were separated on a C18
188 column (Acclaim TM RSLC 120 C18, 2.2 µm 120 A 2.1x100 mm, Dionex bonded silica products)
189 operated at 30°C for a total run time of 20 minutes. The gradient was started with 1% B for 3 minutes

at 0.2 mL.min^{-1}, followed by 39% B. At 14 minutes: the flow was set to 0.4 mL.min^{-1} to reach 99.9% B, followed by 0.48 mL.min^{-1} after 16 minutes. At 16.1 minutes, solvent B was reduced to 1% and the flow to 0.2 ml.min^{-1} at 19.1 minutes to end the run. The spectrometer was used in positive ion mode, with a spectra rate of 2 Hz and a mass range from 30 to 1000 Da. The capillary voltage was set at 2500 V, the nebulizer at 2 Bars and the dry gas at 8 L.min^{-1}, with a dry temperature of 200°C. Fragments were obtained *via* broad-band collision-induced dissociation (bbCID) with a MS/MS collision energy set at 30eV. Poplar leaf extracts were also analyzed using an in-house method for plant extracts as described in Villette et al., (2018), to confirm the MALDI identifications by comparison of retention times and MS/MS profiles between samples and commercially available standards.

2.11. LC-Q-TOF-HRMS data processing

Raw formula annotations and tentative identifications in water, sludge and plant extracts were performed using Metaboscape 3.0 (Bruker) and TASQ 1.4 (Bruker) software, already used by Olmo-García et al., (2018) and Bergé et al., (2018) respectively. In TASQ, a database of 2204 drugs and pesticides was used to annotate ions in a targeted way based on the retention time, m/z value, mSigma and qualifier ions. In Metaboscape, all adduct forms were grouped to form a "bucket", representing one single metabolite feature used for annotations. An intensity threshold of 10 000 was applied for the extraction of metabolite features, which corresponds to a cutoff above 10 times the noise level in our experimental conditions, as already described in the literature (Gago-Ferrero et al., 2018). The untargeted annotations were performed with a criterion of mass deviation (Δm/z) under 3ppm and mSigma value under 30 to assess the good fit of the isotope pattern. The smart Formula tool was applied to perform raw formula annotations using C, H, N, O, P, S, Cl, I, Br and F elements because they are often found in industry chemicals. Tentative identifications were performed using analyte lists created from the toxic exposome database (http://www.t3db.ca/), FooDB (http://foodb.ca/), EU Reference Laboratories for Residues of Pesticides (http://www.eurl-pesticides.eu), Phenol Explorer (http://phenol-explorer.eu/), Scientific Working Group for the Analysis of Seized Drugs (http://www.swgdrug.org/), TargetScreener (Bruker), LIPID MAPS (http://www.lipidmaps.org/), Norman Network (https://www.norman-network.net/), PlantCyc (https://www.plantcyc.org/), KNapSAcK (http://kanaya.naist.jp/KNApSAcK/) and SwissLipids (http://www.swisslipids.org/).The Schymanski classification (Schymanski et al., 2014) was used to assess the level of identification obtained, and is a reference cited in the literature (for example, Bergé et al., (2018)). Metabolite features annotated with only a raw formula were considered annotated (level 4 of the Schymanski classification: unequivocal molecular formula based on MS isotopes/adducts). Metabolite features annotated with a raw formula and a name were considered tentatively identified (level 3 of the Schymanski classification) and manually sorted into 11 categories: personal care products, animal metabolism, drugs, industry toxics, lipid metabolism, other toxics, pesticides, phthalates, primary

metabolism, plant metabolism, uncategorized. The metabolites of 67 common drugs were predicted using Metabolite Predict 2.0 (Bruker), and used as an analyte list to search for drug metabolites in the samples. Commercial standards of 3-ethoxypropylamine, adenine, lyso PC 16:0, pheophorbide A, D-salicin and piperidine were successfully used to confirm the tentative identifications obtained from MSI experiments by comparison of the retention time and MS/MS profiles (when available) of the commercial standards and the ions found in the plant extract (Level 1 of the Schymanski classification).

2.12. MSI sample preparation

Frozen leaves were embedded in M-1 matrix (Thermo Scientific) for cryosectioning at -20°C. Leaves were cut at a thickness of 30 µm on a transverse plane and sections were deposited on ITO-coated slides (Bruker). Sections were coated with α-cyano-4-hydroxyconnamic acid (HCCA, Sigma Aldrich) imaging matrix at 7 $g.L^{-1}$ in 50:50 MeOH:H_2O, 0.2% TFA (Sigma Aldrich) using the ImagePrep spotter (Bruker). The whole process is depicted in Fig. S1. Five replicates of each sample type were prepared and analyzed.

2.13. MSI analysis

MALDI imaging acquisition was performed on a SolariX XR 7T spectrometer (Bruker) in MS positive ion mode using a mass range of 50-1000Da, with a transient size of 2M. On-line calibration was performed using the matrix peaks as reference masses. The laser power was set to 18% with a small focus, 50 shots and a frequency of 1000Hz. The raster width was set to 50 µm. Teaching of the points and definition of the regions of interest were performed using flexImaging 5.0 (Bruker). Data acquisition was performed using ftmsControl 2.2.0 (Bruker).

2.14. MSI data processing

Data obtained from MALDI imaging analysis were treated using SCiLS Lab2016b software as already shown in Halade et al., (2018). Total ion count normalization was applied before each statistical analysis. The segmentation pipeline was used to check for differences between control and polluted leaves, and then discriminative values were searched for using the software tool. The m/z intervals obtained were annotated using the Metaspace online platform (http://metaspace2020.eu)with the HMDB, CHEBI and SwissLipids databases. Metaboscape software (Bruker) was used to complete these annotations using the same analyte lists as described above, with a criterion of mass deviation (Δm/z) under 3 ppm. As described for LC-Q-TOF HRMS data processing,metabolite features annotated with only a raw formula were considered annotated, while metabolite features annotated

with a raw formula and a name were considered tentatively identified. Drug metabolites were also searched for, using the analyte list described above from Metabolite Predict 2.0 (Bruker).

2.15. Statistical analysis

Statistical analysis of the MALDI imaging data was performed with SCiLS Lab 2016b software using the statistical tools provided to perform a spatial segmentation, a principal component analysis (PCA) and to search for discriminative values. The spatial segmentation analysis is a pipeline that performs successive steps: find peaks, peak alignment to maxima, spatial denoising, bisecting k-means. The bisecting k-means step is a clustering method that allows the iterative division of a set of spectra into two maximally different sets of spectra, permitting the segmentation of imaging datasets to visually identify differential regions according to their spectral patterns. This tool is explained in SCiLS Lab application note #6 available on the SCiLS Lab website (https://scils.de/mediacenter/), and for further review, also see Alexandrov et al., (2010); Alexandrov and Kobarg, (2011). PCA applied to MALDI imaging provides a scores plot where each score represents a spectrum and each loading represents a peak (for further review, see Klerk et al., (2007). The plot shown in Fig. 2C provides an overview of the spectra found in each type of sample, control and polluted leaves. Use of the receiver operation characteristic (ROC) curve allows the identification of discriminative values by attributing an area under the curve (AUC): values with an AUC near 0 or 1 were considered to be representative of one or the other group of samples, respectively. Metabolite features with an (AUC)>0.75 were considered specific to the polluted poplar leaves, while metabolite features with an AUC<0.39 were considered specific to the control poplar leaves. These threshold values were calculated by the software to be relevant in the case of this dataset. For further details on the interpretation of AUC values, see SCiLS Lab application note #5 available on the SCiLS Lab website (https://scils.de/mediacenter/).

Statistical analysis of pigments, hormones and stress-related molecule contents in plant extracts were performed using R version 3.3.2 (2016-10-31) Sincere Pumpkin Patch. A Wilcoxon rank-sum test was used with *p*-value thresholds of 0.05 (ingle asterisk) and 0.01 (double asterisk).

3. Results and discussion

3.1. General overview of water, sludge and plant contents

Three compartments of the environment were investigated using a nontargeted approach to gain an overview of the diversity of micropollutants that can be found at the exit of a water treatment facility. Water, sludge and black poplar leaves were sampled and extracted to analyze their contents using LC coupled to high HRMS. The results (Fig. 1) revealed that part of the compounds detected in the different samples were common to the three compartments of the environment. Conversely, some compounds were exclusively specific to only one compartment or two compartments (Fig. 1, A).

Tentative identifications (Level 3 of the Schymanski classification (Schymanski et al., 2014)) were obtained by comparison with the public databases listed in section 2.11.Upon closer examination of the tentative identifications, 11 types of manually curated compounds could be found in all three compartments, in different proportions depending on the compartment analyzed (Fig. 1, B, C, D). Predictably, compounds categorized as animal metabolism, lipid metabolism, primary metabolism and plant metabolism could be found in all compartments of the environment. Interestingly, micropollutants categorized in personal care products, drugs, industry toxics, other toxics, pesticides and phthalates could also be found in all the compartments, showing that these molecules were capable of spreading in the environment, as previously demonstrated (Carvalho et al., 2014). The novelty of the present analysis is the demonstration of this phenomenon using a nontargeted approach in a spontaneous species, black poplar (*P. nigra*), which was previously mostly studied in a targeted way in crops or edible plants (Prosser and Sibley, 2015; Wang et al., 2018). Moreover, we were able to show a specific tissue localization of these micropollutants in poplar leaves using mass spectrometry imaging (MSI) (Fig. 2).

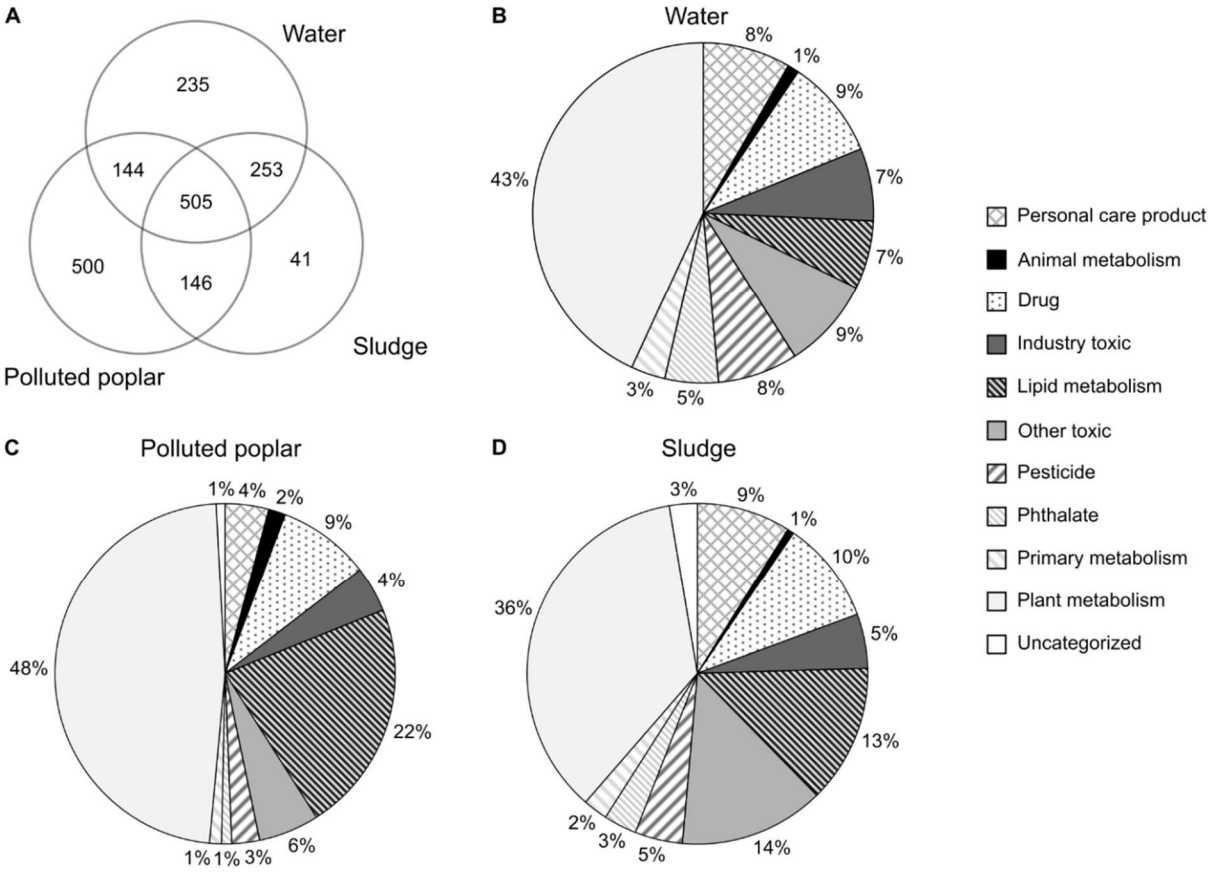

Fig. 1. Profiling of polluted poplar leaves, water and sludge content using LC-HRMS. Polluted poplar leaves, water and sludge show specific but also common metabolite features (**A**). Tentatively annotated compounds (Level 3 of the Schymanski classification) were manually sorted in 11 major classes, revealing the metabolic profile of each compartment of the environment (**B**, **C**, **D**). A, Specific

and common metabolite features between the tree compartments; B, water profiling; C, polluted poplar leaves profiling; D, sludge profiling.

3.2. Mass spectrometry imaging of Populus nigra leaves

MSI was used to investigate the metabolic profile of the leaves from a poplar that was chronically exposed to low doses of micropollutants. The implementation of a control plant growing at the same study site but only with access to rain water allowed a differential analysis to identify the molecules that were present mostly in one or the other condition, namely, control or polluted black poplar leaves (Fig. 2). A segmentation analysis revealed specific metabolic profiles in the control and polluted leaves, as shown by the dark and light blue colors, respectively, in Fig. 2, B. The yellow segments found in control and polluted leaves could not be correlated with specific tissues and were not investigated because they were common to control and polluted leaves. The differential metabolic profile observed between control and polluted leaves was confirmed by principal component analysis (PCA, Fig. 2 and Fig. S2), which resulted in the two first components separating the control (component 1) and polluted (component 2) leaves (Fig. 2, C). The PCA scores plot shows the spectra found in both samples (red, control; green, polluted). The causative metabolite features were further investigated and could be either annotated with a raw formula, tentatively identified (Table S1) or identified. The tentatively identified level consisted of a name associated with the raw formula, while the identified level was confirmed using a commercial standard (Fig. S5) as described in Schymanski et al., (2014). The tentative identifications could be manually sorted into distinct categories: micropollutants or plant metabolites. Among the tentatively identified metabolite features, 6 were confirmed by comparing the retention time and MS/MS profiles when available, in the samples and commercial standards (Fig. S5). In this way, 3-ethoxypropylamine, adenine, lyso PC 16:0, pheophorbide a, salicin and piperidine were confirmed. For D-salicin and piperidine, only the retention times were available, as no MS/MS spectra could be acquired in the leaf extract analysis. As metabolic processes occur in plants, drug metabolites were also searched for and could be tentatively identified in poplar leaves (Table S1).

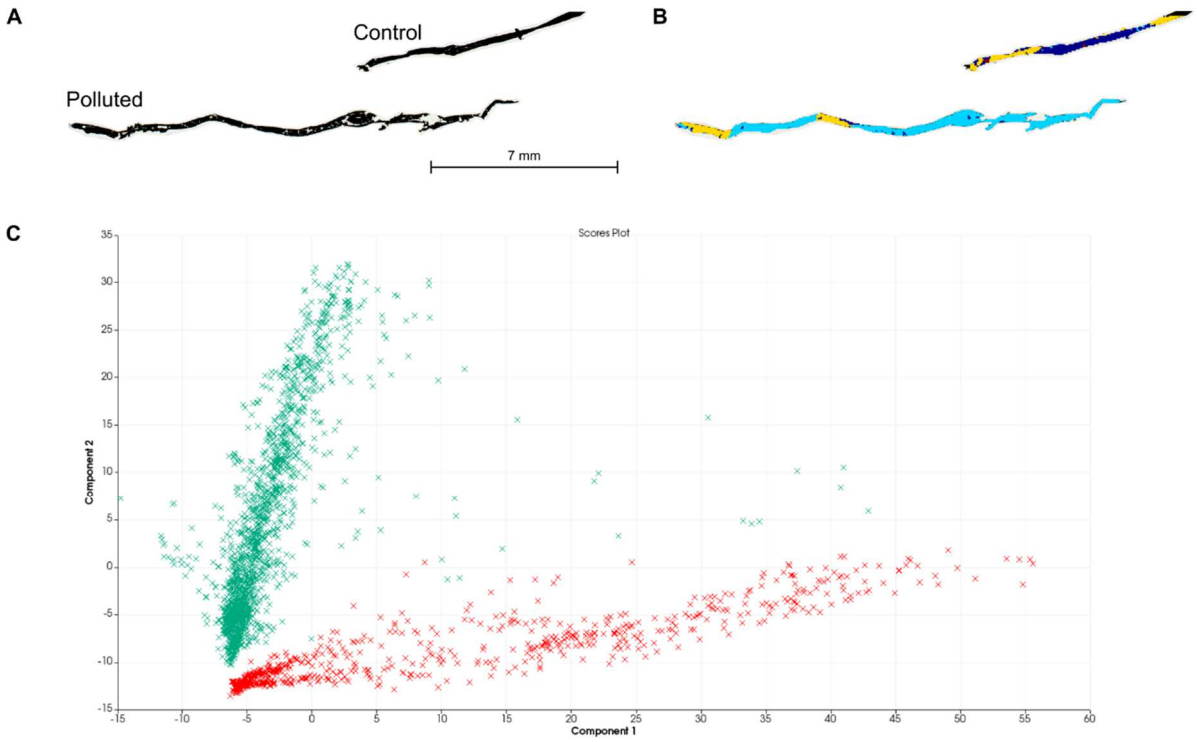

Fig. 2. Overview of the main differences between control and polluted poplar leaves. Control and polluted leaves could be distinguished by a statistical analysis, which shows two specific metabolic patterns. Component 1 is closely related to the control leaves, while component 2 is related to the polluted leaves. **A**, Optical image; **B**, egmentation result; **C**, scores plot of the principal component analysis, with each point representing a spectrum; red, component 1 (related to control); green, component 2 (related to polluted).

Micropollutants were found to be mostly localized in the peripheral regions of the leaf, showing a specific pattern (Fig. 3), while plant metabolites could be found in all regions of the leaves (Fig. 4). Such tissue specific localization has been observed previously in other plants: flavonoids have been shown to be stored in the leaf epidermis in *Ginkgo biloba* (Li et al., 2018), or a spatial metabolites compartmentalization has been revealed in soybean root nodules in response to rhizobacteria (Veličković et al., 2018) using the MSI technique. Micropollutants could also be detected in *Phragmites australis* (Petrie et al., 2018) and ibuprofen has been shown to be stored and metabolized in vacuoles or cell walls (He et al., 2017). These findings suggest that the plant guides micropollutants towards the peripheral tissues of the leaf for storage, which could be the most efficient manner for the plant to confine potentially toxic molecules. The aggregation of compounds on the leaf surface of *Populus trichocarpa* has been previously observed by MSI, revealing active processes that occur in peripheral tissues (Kulkarni et al., 2018). The physico-chemical properties of these molecules could not be correlated with a specific chemistry or logical explanation for such a specific tissue localization (Table S2). According to a previous study (Zhang et al., 2014), molecules with logP values between 0.5 and 3 appear to be efficiently taken up by plants, which was also observed for the molecules highlighted in this study.

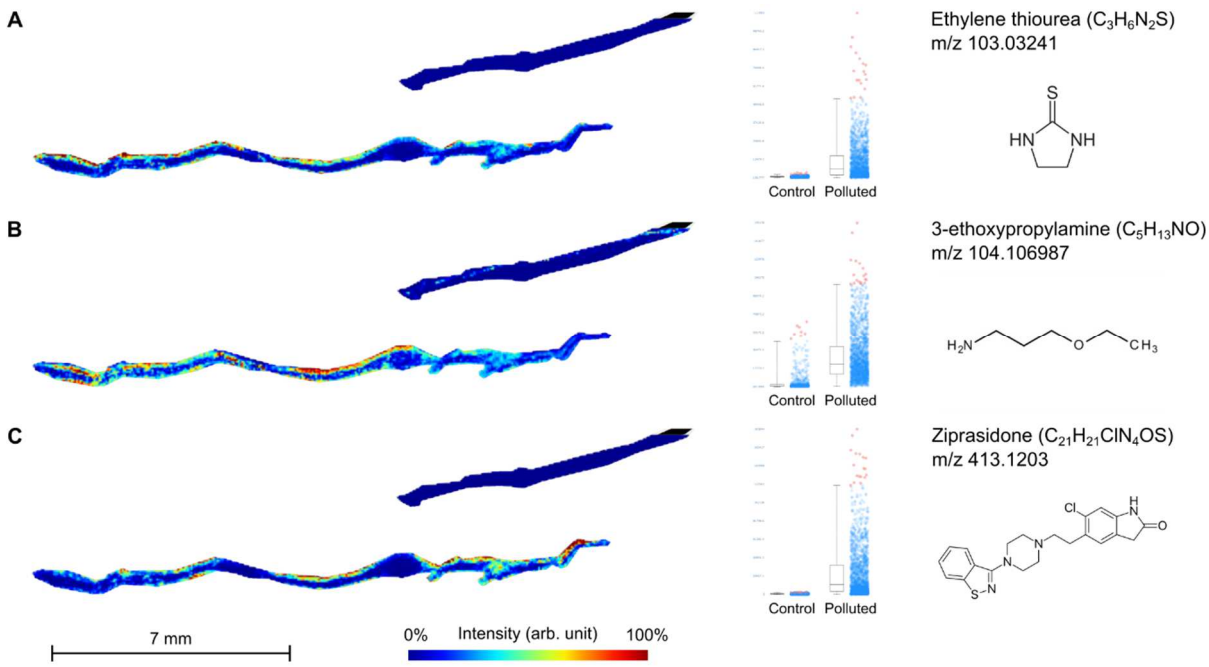

Fig. 3. Micropollutants annotated in poplar leaves. Some differential metabolite features were annotated as micropollutants used as pesticides (**A**), personal care product derivatives (**B**) or drugs (**C**). The images (left) show a preferential localization in the peripheral tissues of the polluted leaves. Boxplots confirm that these metabolite features are differential between control and polluted leaves. A, Ethylene thiourea; B, 3-ethoxypropylamine; C, ziprasidone. Intensity is presented as an arbitrary unit and represented by a color gradient. The chemical properties of ethylene thiourea, 3-ethoxypropylamine and ziprasidone are shown in Table S2. Replicates are shown in Fig. S3.

One could expect a specific phenotype associated with this storage, and therefore we performed transmission electron microscopy observations of the control and polluted poplar leaves (Fig. S6). We could not identify any characteristic features of the tissue organization or organ shape: chloroplasts, mitochondria, nuclei and cell phenotypes were the same in control and polluted leaves. Thus, the plant was able to cope with the micropollutant accumulation. However, the tentative identification of differential metabolite features highlighted a higher amount of stress-related plant metabolites in the polluted leaves, with no physico-chemical properties explaining their tissue localization. Lyso PC 16:0 is a phosphatidylcholine; this class of molecules has been shown to be induced during the plant response to salt stress (Sarabia et al., 2018), suggesting a stress response from the polluted poplar. Pheophorbide a is a chlorophyll a catabolite, thus revealing a pigment degradation in the polluted leaves. Parween et al., 2013 have also observed that the chlorophyll content is affected in mung beans (*Vigna radiata*) exposed to a pesticide.

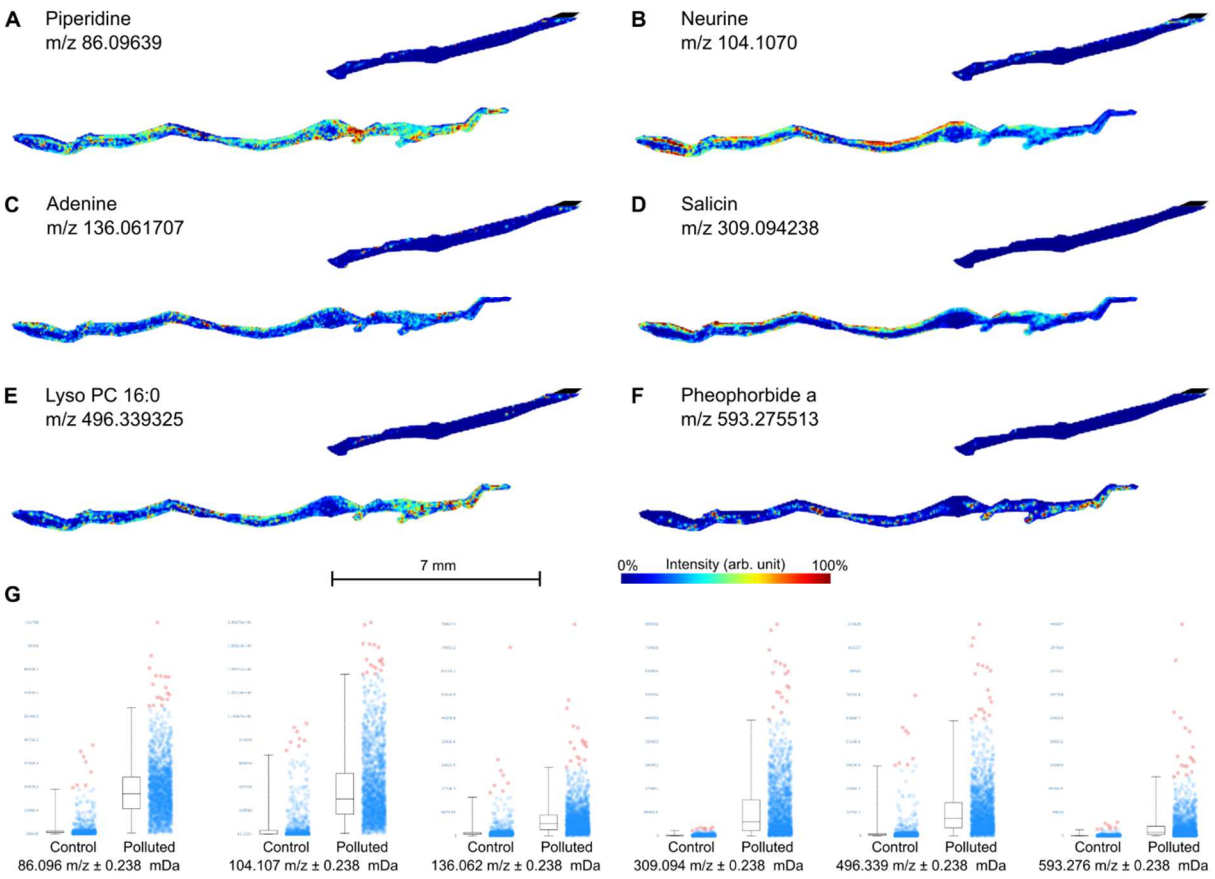

Fig. 4. Plant metabolites annotated in poplar leaves. Plant metabolites were annotated in poplar leaves and appear to be more generally distributed. Neurine (**B**) and salicin (**D**) are mostly found in peripheral tissues, pheophorbide a (**F**) is localised in inner tissues, and other metabolites are found in the whole leaves. Boxplots (**G**) confirm that these metabolite features are differential between control and polluted leaves. Intensity is presented as an arbitrary unit and represented by a color gradient. The chemical properties of piperidine, neurine, adenine, salicin, lyso PC 16:0 and pheophorbide a are presented in Table S2. Replicates are shown in Fig. S4.

3.3. Targeted plant metabolite analysis in Populus nigra leaves

As the plant metabolites induced in polluted leaves are related to plant stress and pigment degradation (Eckardt, 2009; Fernandes et al., 2018), a targeted analysis of pigments, hormones and azelaic acid was performed (Fig. 5). A degradation product of chlorophyll a was more abundant in polluted leaves, and thus we can expect that the plant produced more chlorophyll to counter this loss, with more rapid turnover of chlorophyll a production and degradation. This hypothesis is supported by the finding that chlorophyll a content is higher in polluted leaves (Fig. 5), with no significant differences observed for chlorophyll b and carotenoids. Additionally, no metabolites of these pigments were tentatively annotated. Hormones are the first signals to be emitted by plants in response to a diversity of biotic and abiotic stresses. In polluted leaves, benzoic acid (BA), salicylic acid (SA), azelaic acid (AzA), indole-butyric acid (IBA) and gibberellin A7 (GA_7) were induced compared with the control plant, while cis-OPDA (a jasmonic acid precursor) and abscisic acid (ABA) contents were reduced. The detection of high amounts of IBA in the polluted poplar is not surprising if we consider that this plant

has a generally higher metabolic turnover. Indeed, IBA is involved in the abiotic stress response (Tognetti et al., 2010) -which could be mediated by micropollutant accumulation- but also in plant growth (Strader and Bartel, 2011), which is favored by the continuous presence of water in the growing area (Nuel et al., 2018). Thus, the plant would attempt to produce more biomass to counter the possible loss due to micropollutant accumulation in peripheral tissues. Indeed, the leaves of the polluted poplar were larger than those of the control (Fig. S7), with an average area of 2.5±0.40 cm^2 for the control leaves and 5.56±0.60 cm^2 for the polluted leaves. This hypothesis is strengthened by the detection of higher levels of gibberellin A_7 (GA_7), a hormone involved in the promotion of growth and cell elongation (Katsumi and Kawamura, 1980). Azelaic acid (AzA), a stress-related molecule (Jung et al., 2009), was also measured and found to be more abundant in polluted leaves. Azelaic acid (AzA) is known to be involved in systemic acquired resistance (SAR), inducing the production of salicylic acid, which is consistent with the higher levels of this hormone found in the polluted leaves. In the SAR context, jasmonic acid (JA) and SA are antagonistic: JA acts as a signaling molecule, while SA accumulation allows the establishment of systemic immunity (Jung et al., 2009; Thaler et al., 2012). After exposure to micropollutants, a SAR-like reaction could occur and explain the reduced levels of JA precursor cis-OPDA in polluted leaves, and the fact that no difference in JA content was observed between control and polluted leaves. Indeed, SA has been described as a regulatory signal in response to a variety of abiotic stresses: drought, high salinity, chilling, heavy metal exposure and heat (Gómez-Cadenas et al., 2014). In the case of a SAR response, long term accumulation of SA is not necessary (Jung et al., 2009). Thus, if the reaction to micropollutants accumulation is similar to a SAR response, we could hypothesize that the polluted poplar is responding to a chronic exposure and needs to maintain high levels of stress-associated metabolites to support consistent defense mechanisms. This response resembles the induced resistance used in agricultural practices to control crop diseases: the application of natural extracts or synthetic chemicals (biotic and abiotic elicitors) triggers a biological response from the plant, leading to induced resistance (Walters et al., 2013). In *Avena fatua*, herbicides have been described to prime redox and phosphoproteome changes similar to those occurring during SAR response (Burns et al., 2018). We can hypothesize that micropollutants from the water might have a role as activators of the poplar stress response highlighted in this study.

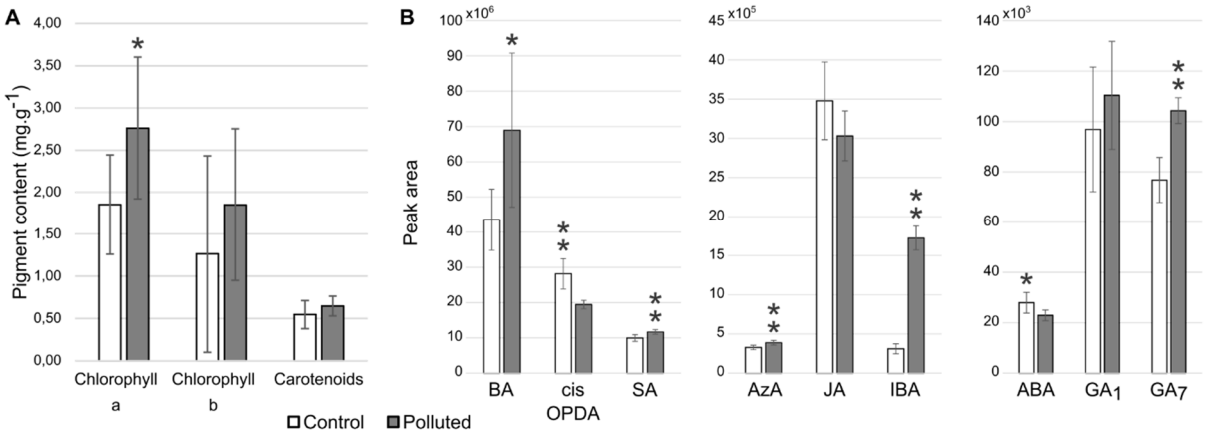

Fig. 5. Pigments, hormones and azelaic acid profiling in control and polluted poplar leaves. Pigment analysis revealed more chlorophyll a in the polluted leaves (*p*-value 0.03792). Control leaves contain more ABA and cis-OPDA (*p*-values 0.02067 and 0.006993, respectively). Polluted leaves show higher amounts of BA, SA, GA_7, Aza and IBA (*p*-values 0.0141, 0.001348, 0.00015554, 0.002953 and 0.000931, respectively). **A**, Average pigment content in $mg.g^{-1}$ fresh weight; **B**, Hormones and stress-related compound content expressed as peak areas. JA, jasmonic acid; BA, benzoic acid; cis-OPDA, cis-(+)-12-oxo-phytodienoic acid; SA, salicylic acid; $GA_{1,\ 7}$, gibberellins 1 and 7; Aza, azelaic acid; IBA, indole butyric acid; ABA, abscisic acid. Error bars represent the standard deviation. Statistical analysis was performed using a Wilcoxon rank-sum test.

The toxicity of pharmaceuticals to plants has been discussed by Carvalho et al., (2014) and recently reviewed by Christou et al., (2018) because of their wide and continuous spreading in all areas of the environment. Conversely, a constant low dose of micropollutants could also induce hormesis and increase biomass production (Agathokleous et al., 2018; Migliore et al., 2000), but this hypothesis is not consistent with the increased accumulation of degradation products in polluted leaves. Interestingly, piperidine has been found in higher amounts in polluted poplar. This metabolite is a toxic alkaloid that is produced by plants to avoid consumption by herbivores (Castells et al., 2005). Butler and Trumble, (2008) reviewed the literature on plant-insect interactions in the context of polluted plants and described polluted plants as better hosts for herbivore insects. This finding was demonstrated in the case of air pollution, but we can expect that water pollutants would have the same effects. Thus, polluted poplar is more attractive to insect herbivores and produces more piperidine as a defense mechanism. Piperidine is also an industry derivative that is used, for example, for the synthesis of drugs or pesticides (Shaw et al., 2015), and might be accumulated by plants from the environment. Personal care products, pesticides, drugs, phthalates, industry toxics and other toxics could be found in different proportions in water, sludge and plants. However, the prominent categories were always the same among the different matrices and were found with a rather equivalent distribution. Thus, micropollutants are spreading in all areas of the environment. When sorting the tentative identifications, difficulty was encountered because plant metabolites are found in food and used in drugs and personal care products. Thus, for plant metabolites generated by human activities, whether they were accumulated by poplar leaves from the water or sludge or naturally produced in

higher amounts in the plant remained unclear. A similar situation was observed for salicin, which occurs naturally in poplar but is also used as an anti-inflammatory drug (Mahdi, 2010). Salicin from the drug is metabolized into salicylic acid in the human digestive tract, and it is described to be easily degraded in the environment (Hijosa-Valsero et al., 2016). Therefore, it wass also difficult to determine if the increase in salicylic acid in polluted leaves is due to production by the plant or uptake from the water. The same holds true for benzoic acid (BA), a commonly used compound in cosmetics, which was found to be more abundant in polluted leaves. Additionally, IBA is used as a plant growth regulator in agriculture and might have been detected in higher amounts because of its use in nearby fields.

An important aspect when comparing water, sludge and plants is the concentration effect that can occur in the different matrices. Indeed, all samples were collected on the same day, but sludge and poplar leaves could have accumulated molecules over a long period, while the water was fresh from the day. An important concentration effect occurs in the leaves, while the molecules are more diluted in sludge and even more in water that are present in larger amounts in the environment, with the constant renewal of the water. This phenomenon is especially true in the case of Falkwiller village where rain water is collected along with urban wastewater. Despite a concentration step during the extraction process, it is impossible to consider the different samples as equivalent. Therefore, it is difficult to follow the exact same micropollutants from one sample type to the other. Moreover, some compounds are not stable in plants and can be degraded to avoid toxicity or for reuse by plant metabolism (Marsik et al., 2017). In this study, metabolites of aceclidine, telmisartan and haloperidol could be annotated in poplar leaves (Table S1), but the identification could not be confirmed because of the lack of standards for these molecules.

3.4. Methodological assessment

Commercial labelled standards of drugs were used as a mixture pooled to water and sludge matrices to assess the repeatability of the extraction process and to define the limits of detection (LOD) and quantification (LOQ), as described in Boleda et al., (2013). Repeatability was studied by analysis of the standard deviation measured for the peak areas of the internal standards in the two matrices (sludge and water). The coefficients of variation (CV) observed were included in a range from 1 to 31% of the standard deviations (Table S3). These values were in accordance with Boleda et al., (2013), except for one among seven standards that showed higher CV values for unexplained reasons. The limits of detection reached approximately 1 $\mu g.mL^{-1}$ (Table S4 and Fig. S8). Therefore, in the original matrices (in the environment, before sample concentration), the detected molecules can be considered to be present at least at 0.1 $\mu g.g^{-1}$ (fresh weight) in the sludge matrix (10 g used for the analysis) and 0.02 $\mu g.mL^{-1}$ in the water matrix (50 mL used for the analysis). We cannot exclude the possibility that other

molecules were present in the different matrices at a lower dose and therefore could not be detected. As observed for sildenafil, it is also possible that some molecules were not detected irrespective of their concentration, potentially because, for example, they were not easily ionized.

4. Conclusions

In this study, we demonstrated that micropollutants are still detectable and are spreading in the different areas of the environment after water treatment. We analyzed the metabolic profile of black poplar (*P. nigra*) leaves using high-resolution MSI, which showed the accumulation of micropollutants and a stress response from the plant. We could correlate metabolite classes with a specific tissue localization. In general, compounds that might originate from industry chemistry (drugs, pesticides, personal care products, toxics, etc.) appeared to be sequestered in the peripheral tissues close to the epidermis, while plant metabolites were more generally distributed. We could show a specific tissue localization of a pesticide metabolite (ethylene thiourea), an intermediate of personal care product production (3-ethoxypropylamine) and potentially drug derivatives. Along with this specific localization of micropollutants, we demonstrated a response of the plant that was chronically exposed to micropollutants, with higher amounts of degradation products (neurine, pheophorbide a) and a plant response designed to increase biomass production as a survival mechanism. As plants accumulate micropollutants throughout their life span, a low dose at a time point can become a high dose at the scale of a living organism. If this is true for a plant, it should also be true for any living organism, including other plant species, crops, wild and farmed animals, as well as humans. Water is an essential resource for human life, but it is also a carrier of micropollutants, which we have shown cannot always be treated and completely eliminated. Thus, these contaminants spread in the environment and in living organisms, and cause tissue damages and stress. This study provides an overview of environmental contamination by treated water and raises questions regarding water quality for a sustainable environment for living organisms.

In future analyses, we plan to investigate the whole plant to decipher the distribution of micropollutants in the different organs. As highlighted by Jansson and Douglas, 2007, poplars are well known to interact with fungus and bacteria as endophytes, which provide the plant with nutrients. We are also interested in the roles of microorganisms, which could participate in micropollutants degradation or act as helpers for their uptake from the environment.

Acknowledgments: We acknowledge the Agence de l'Eau Rhin Meuse (AERM) and the village of Falkwiller for access to the wetland.

Author contributions: C.V. conducted the LC-Q-TOF-HRMS and mass spectrometry imaging (MSI) data acquisition, analyzed the plant sample data, prepared the figures and wrote the manuscript. L.M. performed the water and sludge sample preparation and data analysis, prepared the figures and discussed the manuscript. J.D. participated in the acquisition of the imaging data. J.Z. performed the targeted mass spectrometry acquisitions. M.E. performed the microscopy experiments. D.H. contributed to the design of the experiments and sample preparation, discussed the results and revised the manuscript.

Competing interests: The authors declare they have no competing interests.

Data and materials availability: Data and materials are fully available from the corresponding author upon reasonable request.

Supplementary Materials

Data file S1. Tentative identifications of metabolite features detected using LC-Q-TOF-HRMS in plant, water and sludge samples.

References and Notes

Adeel, M., Song, X., Wang, Y., Francis, D., Yang, Y., 2017. Environmental impact of estrogens on human, animal and plant life: A critical review. Environ. Int. 99, 107–119. https://doi.org/10.1016/j.envint.2016.12.010

Agathokleous, E., Kitao, M., Calabrese, E.J., 2018. Human and veterinary antibiotics induce hormesis in plants: Scientific and regulatory issues and an environmental perspective. Environ. Int. 120, 489–495. https://doi.org/10.1016/j.envint.2018.08.035

Alexandrov, T., Becker, M., Deininger, S., Wehder, L., Grasmair, M., Eggeling, F. Von, Thiele, H., Maass, P., 2010. Spatial Segmentation of Imaging Mass Spectrometry Data with Edge-Preserving Image Denoising and Clustering research articles 6535–6546.

Alexandrov, T., Kobarg, J.H., 2011. Efficient spatial segmentation of large imaging mass spectrometry datasets with spatially aware clustering 27, 230–238. https://doi.org/10.1093/bioinformatics/btr246

Anderson, D.M.G., Carolan, V.A., Crosland, S., Sharples, K.R., Clench, M.R., 2010. Examination of the translocation of sulfonylurea herbicides in sunflower plants by matrix-assisted laser desoprtion/ionisation mass spectrometry imaging. Rapid Commun. Mass Spectrom. 24, 3309–3319. https://doi.org/10.1002/rcm.4767

575 Bergé, A., Buleté, A., Fildier, A., Mailler, R., Gasperi, J., Coquet, Y., Nauleau, F., Rocher,
576 V., Vulliet, E., 2018. Non-target strategies by HRMS to evaluate fluidized micro-grain
577 activated carbon as a tertiary treatment of wastewater. Chemosphere 213, 587–595.
578 https://doi.org/10.1016/j.chemosphere.2018.09.101
579 Bhandari, D.R., Wang, Q., Friedt, W., Spengler, B., Gottwald, S., Römpp, A., 2015. High
580 resolution mass spectrometry imaging of plant tissues: Towards a plant metabolite atlas.
581 Analyst 140, 7696–7709. https://doi.org/10.1039/c5an01065a
582 Bjarnholt, N., Li, B., D'Alvise, J., Janfelt, C., 2014. Mass spectrometry imaging of plant
583 metabolites-principles and possibilities. Nat. Prod. Rep. 31, 818–837.
584 https://doi.org/10.1039/c3np70100j
585 Boleda, M.R., Galceran, M.T., Ventura, F., 2013. Validation and uncertainty estimation of a
586 multiresidue method for pharmaceuticals in surface and treated waters by liquid
587 chromatography-tandem mass spectrometry. J. Chromatogr. A 1286, 146–158.
588 https://doi.org/10.1016/j.chroma.2013.02.077
589 Burns, E.E., Keith, B.K., Refai, M.Y., Bothner, B., Dyer, W.E., 2018. Constitutive redox and
590 phosphoproteome changes in multiple herbicide resistant Avena fatua L. are similar to
591 those of systemic acquired resistance and systemic acquired acclimation. J. Plant
592 Physiol. 220, 105–114. https://doi.org/10.1016/j.jplph.2017.11.004
593 Butler, C.D., Trumble, J.T., 2008. Effects of pollutants on bottom-up and top-down processes
594 in insect-plant interactions. Environ. Pollut. 156, 1–10.
595 https://doi.org/10.1016/j.envpol.2007.12.026
596 Carvalho, P.N., Basto, M.C.P., Almeida, C.M.R., Brix, H., 2014. A review of plant–
597 pharmaceutical interactions: from uptake and effects in crop plants to phytoremediation
598 in constructed wetlands. Environ. Sci. Pollut. Res. 21, 11729–11763.
599 https://doi.org/10.1007/s11356-014-2550-3
600 Castells, E., Berhow, M.A., Vaughn, S.F., Berenbaum, M.R., 2005. Geographic variation in
601 alkaloid production in *Conium maculatum* populations experiencing differential
602 herbivory by *Agonopterix alstroemeriana*. J. Chem. Ecol. 31, 1693–1709.
603 https://doi.org/10.1007/s10886-005-5921-x
604 Christou, A., Michael, C., Fatta-Kassinos, D., Fotopoulos, V., 2018. Can the pharmaceutically
605 active compounds released in agroecosystems be considered as emerging plant stressors?
606 Environ. Int. 114, 360–364. https://doi.org/10.1016/j.envint.2018.03.003
607 Cotton, J., Leroux, F., Broudin, S., Poirel, M., Corman, B., Junot, C., Ducruix, C., 2016.
608 Development and validation of a multiresidue method for the analysis of more than 500

609 pesticides and drugs in water based on on-line and liquid chromatography coupled to
610 high resolution mass spectrometry. Water Res. 104, 20–27.
611 https://doi.org/10.1016/j.watres.2016.07.075
612 Eckardt, N.A., 2009. A New Chlorophyll Degradation Pathway. Plant Cell Online 21, 700–
613 700. https://doi.org/10.1105/tpc.109.210313
614 Fernandes, C., Figueira, E., Tauler, R., Bedia, C., 2018. Exposure to chlorpyrifos induces
615 morphometric, biochemical and lipidomic alterations in green beans (*Phaseolus*
616 *vulgaris*). Ecotoxicol. Environ. Saf. 156, 25–33.
617 https://doi.org/10.1016/j.ecoenv.2018.03.005
618 Gago-Ferrero, P., Krettek, A., Fischer, S., Wiberg, K., Ahrens, L., 2018. Suspect Screening
619 and Regulatory Databases: A Powerful Combination to Identify Emerging
620 Micropollutants. Environ. Sci. Technol. 52, 6881–6894.
621 https://doi.org/10.1021/acs.est.7b06598
622 Gómez-Cadenas, A., de Ollas, C., Manzi, M., Arbona, V., 2014. Phytohormonal crosstalk
623 under abiotic stress, in: Phytohormones: A Window to Metabolism, Signaling and
624 Biotechnological Applications. pp. 289–321. https://doi.org/10.1007/978-1-4939-0491-4
625 Guidi, W., Piccioni, E., Bonari, E., 2008. Evapotranspiration and crop coefficient of poplar
626 and willow short-rotation coppice used as vegetation filter. Bioresour. Technol. 99,
627 4832–4840. https://doi.org/10.1016/j.biortech.2007.09.055
628 Halade, G. V., Dorbane, A., Ingle, K.A., Kain, V., Schmitter, J.M., Rhourri-Frih, B., 2018.
629 Comprehensive targeted and non-targeted lipidomics analyses in failing and non-failing
630 heart. Anal. Bioanal. Chem. 410, 1965–1976. https://doi.org/10.1007/s00216-018-0863-7
631 He, Y., Langenhoff, A.A.M., Sutton, N.B., Rijnaarts, H.H.M., Blokland, M.H., Chen, F.,
632 Huber, C., Schröder, P., 2017. Metabolism of Ibuprofen by *Phragmites australis*: Uptake
633 and Phytodegradation. Environ. Sci. Technol. 51, 4576–4584.
634 https://doi.org/10.1021/acs.est.7b00458
635 Hijosa-Valsero, M., Reyes-Contreras, C., Domínguez, C., Bécares, E., Bayona, J.M., 2016.
636 Behaviour of pharmaceuticals and personal care products in constructed wetland
637 compartments: Influent, effluent, pore water, substrate and plant roots. Chemosphere
638 145, 508–517. https://doi.org/10.1016/j.chemosphere.2015.11.090
639 Jakovljević, T., Cvjetko Bubalo, M., Orlović, S., Sedak, M., Bilandžić, N., Brozinčević, I.,
640 Radojčić Redovniković, I., 2014. Adaptive response of poplar (*Populus nigra* L.) after
641 prolonged Cd exposure period. Environ. Sci. Pollut. Res. 21, 3792–3802.
642 https://doi.org/10.1007/s11356-013-2292-7

643 Jansson, S., Douglas, C.J., 2007. *Populus* : A Model System for Plant Biology. Annu. Rev.
644 Plant Biol. 58, 435–458. https://doi.org/10.1146/annurev.arplant.58.032806.103956
645 Jung, H.W., Tschaplinski, T.J., Wang, L., Glazebrook, J., Greenberg, J.T., 2009. Priming in
646 Systemic Plant Immunity 324, 89–92.
647 Katsumi, M., Kawamura, N., 1980. Physiological effects of cotyledons on gibberellin-induced
648 cucumber hypocotyl elongation. Plant Cell Physiol. 21, 1439–1448.
649 Klerk, L.A., Broersen, A., Fletcher, I.W., Liere, R. Van, Heeren, R.M.A., 2007. Extended
650 data analysis strategies for high resolution imaging MS : New methods to deal with
651 extremely large image hyperspectral datasets 260, 222–236.
652 https://doi.org/10.1016/j.ijms.2006.11.014
653 Kulkarni, P., Dost, M., Bulut, Ö.D., Welle, A., Böcker, S., Boland, W., Svatoš, A., 2018.
654 Secondary ion mass spectrometry imaging and multivariate data analysis reveal co-
655 aggregation patterns of *Populus trichocarpa* leaf surface compounds on a micrometer
656 scale. Plant J. 93, 193–206. https://doi.org/10.1111/tpj.13763
657 Lagarrigue, M., Caprioli, R.M., Pineau, C., 2016. Potential of MALDI imaging for the
658 toxicological evaluation of environmental pollutants. J. Proteomics 144, 133–139.
659 https://doi.org/10.1016/j.jprot.2016.05.008
660 Lee, K.Y., Strand, S.E., Doty, S.L., 2012. Phytoremediation of chlorpyrifos by *Populus* and
661 *Salix*. Int. J. Phytoremediation 14, 48–61.
662 https://doi.org/10.1080/15226514.2011.560213
663 Lee, Y.J., Perdian, D.C., Song, Z., Yeung, E.S., Nikolau, B.J., 2012. Use of mass
664 spectrometry for imaging metabolites in plants. Plant J. 70, 81–95.
665 https://doi.org/10.1111/j.1365-313X.2012.04899.x
666 Li, B., Neumann, E.K., Ge, J., Gao, W., Yang, H., Li, P., Sweedler, J. V., 2018. Interrogation
667 of Spatial Metabolome of *Ginkgo biloba* with High-resolution MALDI and LDI Mass
668 Spectrometry Imaging. Plant. Cell Environ. 1–11. https://doi.org/10.1111/pce.13395
669 Lichtenthaler, H.K., Buschmann, C., 2001. Chlorophylls and carotenoids: measurement and
670 characterization by UV-VIS spectroscopy. Curr. Protoc. food Anal. Chem. F4.3.1-
671 F4.3.8.
672 Mahdi, J.G., 2010. Medicinal potential of willow: A chemical perspective of aspirin
673 discovery. J. Saudi Chem. Soc. 14, 317–322. https://doi.org/10.1016/j.jscs.2010.04.010
674 Marsik, P., Sisa, M., Lacina, O., Motkova, K., Langhansova, L., Rezek, J., Vanek, T., 2017.
675 Metabolism of ibuprofen in higher plants: A model *Arabidopsis thaliana* cell suspension
676 culture system. Environ. Pollut. 220, 383–392.

https://doi.org/10.1016/j.envpol.2016.09.074
Migliore, L., Cozzolino, S., Fiori, M., 2000. Phytotoxicity to and uptake of flumequine used in intensive aquaculture on the aquatic weed, *Lythrum salicaria* L. Chemosphere 40, 741–750. https://doi.org/10.1016/S0045-6535(99)00448-8
Nuel, M., Laurent, J., Bois, P., Heintz, D., Wanko, A., 2018. Seasonal and ageing effect on the behaviour of 86 drugs in a full-scale surface treatment wetland: Removal efficiencies and distribution in plants and sediments. Sci. Total Environ. 615, 1099–1109. https://doi.org/10.1016/j.scitotenv.2017.10.061
Olmo-García, L., Kessler, N., Neuweger, H., Wendt, K., Olmo-Peinado, J.M., Fernández-Gutiérrez, A., Baessmann, C., Carrasco-Pancorbo, A., 2018. Unravelling the Distribution of Secondary Metabolites in *Olea europaea* L .: Exhaustive Characterization of Eight Olive-Tree Derived Matrices by Complementary Platforms (LC-ESI/APCI-MS and GC-APCI-MS). Molecules 23, 1–16. https://doi.org/10.3390/molecules23102419
Parween, T., Jan, S., Mahmooduzzafar, Fatma, T., 2013. Differential response of *Vigna radiata* L. to varied doses of chlorpyrifos. J. Plant Nutr. 36, 1565–1577. https://doi.org/10.1080/01904167.2013.799185
Petrie, B., Rood, S., Smith, B.D., Proctor, K., Youdan, J., Barden, R., Kasprzyk-Hordern, B., 2018. Biotic phase micropollutant distribution in horizontal sub-surface flow constructed wetlands. Sci. Total Environ. 630, 648–657. https://doi.org/10.1016/j.scitotenv.2018.02.242
Prosser, R.S., Sibley, P.K., 2015. Human health risk assessment of pharmaceuticals and personal care products in plant tissue due to biosolids and manure amendments, and wastewater irrigation. Environ. Int. 75, 223–233. https://doi.org/10.1016/j.envint.2014.11.020
Rivas, D., Zonja, B., Eichhorn, P., Ginebreda, A., Pérez, S., Barceló, D., 2017. Using MALDI-TOF MS imaging and LC-HRMS for the investigation of the degradation of polycaprolactone diol exposed to different wastewater treatments. Anal. Bioanal. Chem. 409, 5401–5411. https://doi.org/10.1007/s00216-017-0371-1
Sarabia, L.D., Boughton, B.A., Rupasinghe, T., van de Meene, A.M.L., Callahan, D.L., Hill, C.B., Roessner, U., 2018. High-mass-resolution MALDI mass spectrometry imaging reveals detailed spatial distribution of metabolites and lipids in roots of barley seedlings in response to salinity stress. Metabolomics 14, 1–16. https://doi.org/10.1007/s11306-018-1359-3
Schneider, C.A., Rasband, W.S., Eliceiri, K.W., 2012. NIH Image to ImageJ: 25 years of

711 Image Analysis HHS Public Access. Nat. Methods 9, 671–675.
712 https://doi.org/10.1038/nmeth.2089
713 Schymanski, E.L., Jeon, J., Gulde, R., Fenner, K., Ruff, M., Singer, H.P., Hollender, J., 2014.
714 Identifying small molecules via high resolution mass spectrometry: Communicating
715 confidence. Environ. Sci. Technol. 48, 2097–2098. https://doi.org/10.1021/es5002105
716 Shaw, S.A., Balasubramanian, B., Bonacorsi, S., Cortes, J.C., Cao, K., Chen, B.C., Dai, J.,
717 Decicco, C., Goswami, A., Guo, Z., Hanson, R., Humphreys, W.G., Lam, P.Y.S., Li, W.,
718 Mathur, A., Maxwell, B.D., Michaudel, Q., Peng, L., Pudzianowski, A., Qiu, F., Su, S.,
719 Sun, D., Tymiak, A.A., Vokits, B.P., Wang, B., Wexler, R., Wu, D.R., Zhang, Y., Zhao,
720 R., Baran, P.S., 2015. Synthesis of Biologically Active Piperidine Metabolites of
721 Clopidogrel: Determination of Structure and Analyte Development. J. Org. Chem. 80,
722 7019–7032. https://doi.org/10.1021/acs.joc.5b00632
723 Strader, L.C., Bartel, B., 2011. Transport and metabolism of the endogenous auxin precursor
724 indole-3-butyric acid. Mol. Plant 4, 477–486. https://doi.org/10.1093/mp/ssr006
725 Thaler, J.S., Humphrey, P.T., Whiteman, N.K., 2012. Evolution of jasmonate and salicylate
726 signal crosstalk. Trends Plant Sci. 17, 260–270.
727 https://doi.org/10.1016/j.tplants.2012.02.010
728 Tognetti, V.B., Van Aken, O., Morreel, K., Vandenbroucke, K., van de Cotte, B., De Clercq,
729 I., Chiwocha, S., Fenske, R., Prinsen, E., Boerjan, W., Genty, B., Stubbs, K.A., Inze, D.,
730 Van Breusegem, F., 2010. Perturbation of Indole-3-Butyric Acid Homeostasis by the
731 UDP-Glucosyltransferase UGT74E2 Modulates *Arabidopsis* Architecture and Water
732 Stress Tolerance. Plant Cell 22, 2660–2679. https://doi.org/10.1105/tpc.109.071316
733 Veličković, D., Agtuca, B.J., Stopka, S.A., Vertes, A., Koppenaal, D.W., Paša-Tolić, L.,
734 Stacey, G., Anderton, C.R., 2018. Observed metabolic asymmetry within soybean root
735 nodules reflects unexpected complexity in rhizobacteria-legume metabolite exchange.
736 ISME J. 1–4. https://doi.org/10.1038/s41396-018-0188-8
737 Villette, C., Zumsteg, J., Schaller, H., Heintz, D., 2018. Non-targeted metabolic profiling of
738 BW312 *Hordeum vulgare* semi dwarf mutant using UHPLC coupled to QTOF high
739 resolution mass spectrometry. Sci. Rep. 8. https://doi.org/10.1038/s41598-018-31593-1
740 Walters, D.R., Ratsep, J., Havis, N.D., 2013. Controlling crop diseases using induced
741 resistance: challenges for the future. J. Exp. Bot. 64, 1263–1280.
742 https://doi.org/10.1093/jxb/ert026
743 Wang, J., Xia, K., Waigi, M.G., Gao, Y., Odinga, E.S., Ling, W., Liu, J., 2018. Application of
744 biochar to soils may result in plant contamination and human cancer risk due to exposure

of polycyclic aromatic hydrocarbons. Environ. Int. 121, 169–177. https://doi.org/10.1016/j.envint.2018.09.010

Zhang, D., Gersberg, R.M., Ng, W.J., Tan, S.K., 2014. Removal of pharmaceuticals and personal care products in aquatic plant-based systems: A review. Environ. Pollut. 184, 620–639. https://doi.org/10.1016/j.envpol.2013.09.009

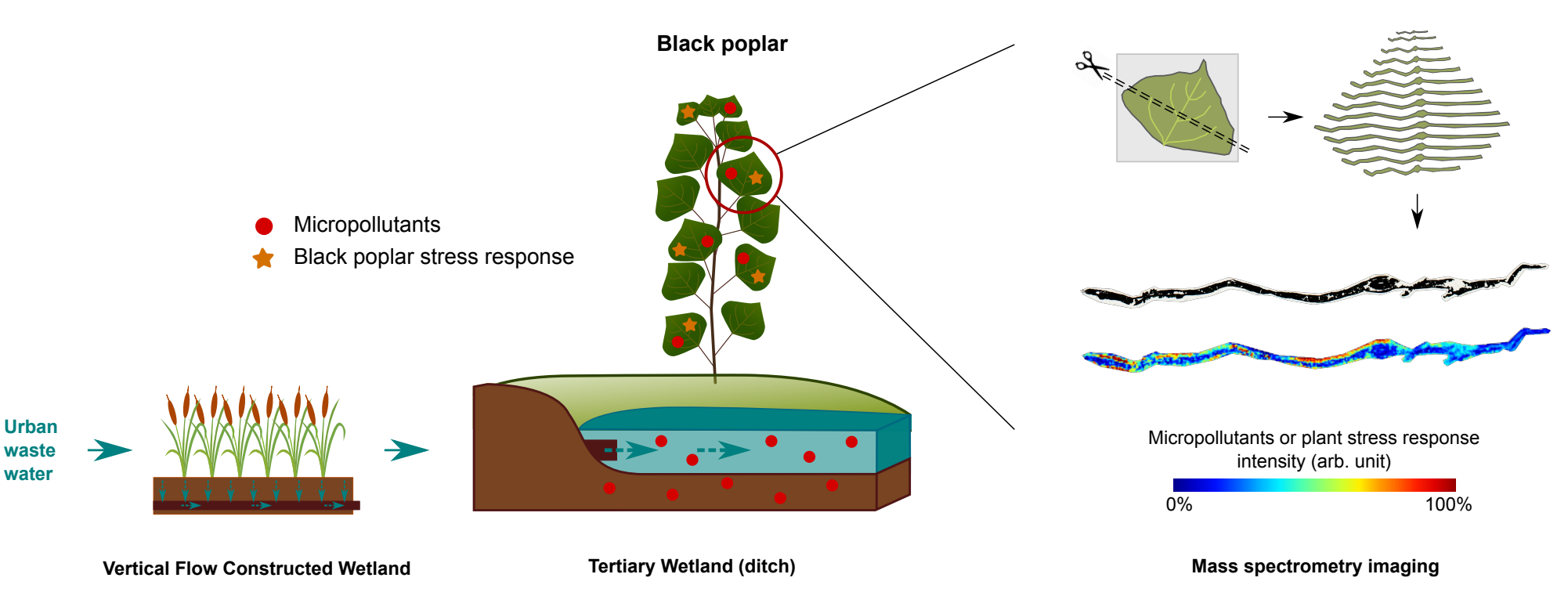
Black poplar
Micropollutants
Black poplar stress response
Urban waste water
Micropollutants or plant stress response intensity (arb. unit)
0%
100%
Vertical Flow Constructed Wetland
Tertiary Wetland (ditch)
Mass spectrometry imaging